REVIEW

National Science Review
11: nwad270, 2024
https://doi.org/10.1093/nsr/nwad270
Advance access publication 31 October 2023

PHYSICS

Special Topic: Challenges to Achieving Room Temperature Superconductivity in Superhydrides under Pressure

Clathrate metal superhydrides under high-pressure conditions: enroute to room-temperature superconductivity

Ying Sun [1,2], Xin Zhong[1,2,*], Hanyu Liu[1,2,3,*] and Yanming Ma[1,2,3,*]

ABSTRACT

Room-temperature superconductivity has been a long-held dream of mankind and a focus of considerable interest in the research field of superconductivity. Significant progress has recently been achieved in hydrogen-based superconductors found in superhydrides (hydrides with unexpectedly high hydrogen contents) that are stabilized under high-pressure conditions and are not capturable at ambient conditions. Of particular interest is the discovery of a class of best-ever-known superconductors in clathrate metal superhydrides that hold the record for high superconductivity (e.g. $T_c = 250$–260 K for LaH_{10}) among known superconductors and have great promise to be those that realize the long-sought room-temperature superconductivity. In these peculiar clathrate superhydrides, hydrogen forms unusual 'clathrate' cages containing encaged metal atoms, of which such a kind was first reported in a calcium hexa-superhydride (CaH_6) showing a measured high T_c of 215 K under a pressure of 170 GPa. In this review, we aim to offer an overview of the current status of research progress on the clathrate metal superhydride superconductors, discuss the superconducting mechanism and highlight the key features (e.g. structure motifs, bonding features, electronic structure, etc.) that govern the high-temperature superconductivity. Future research direction along this line to find room-temperature superconductors will be discussed.

Keywords: clathrate superhydrides, high-temperature superconductivity, high-pressure conditions, crystal structure prediction

[1]Key Laboratory of Material Simulation Methods & Software of Ministry of Education, College of Physics, Jilin University, Changchun 130012, China; [2]State Key Laboratory of Superhard Materials, College of Physics, Jilin University, Changchun 130012, China and [3]International Center of Future Science, Jilin University, Changchun 130012, China

*Corresponding authors. E-mails: zhongxin@calypso.cn; hanyuliu@jlu.edu.cn; mym@jlu.edu.cn

Received 4 June 2023; **Revised** 16 July 2023; **Accepted** 21 September 2023

INTRODUCTION

A superconductor exhibits two characteristic physical properties when cooled below its superconducting critical temperature (T_c) where electrical resistance vanishes [1] and magnetic flux fields are expelled from the bulk [2]. Since the first discovery of superconductivity below 4.2 K in solid mercury in 1911, tremendous efforts have been paid to the goal of achieving superconductors that work at ever higher temperatures for practical applications (see Fig. 1 below). Room-temperature superconductors are yet to be achieved and remain a century-long-held dream of mankind.

Intensive superconductivity research has been devoted to the investigation of two families of so-called 'unconventional' cuprate and iron-based superconductors, whose superconducting mechanism on the electron pairing is not believed to be mediated by the exchange of phonons [3–6]. In these activities, the highest T_c of 133 K at ambient pressure [3] was attained in a Hg–Ba–Ca–Cu–O cuprate material whose T_c was further promoted to 164 K at a high-pressure condition of 31 GPa [4,5], setting the record for T_c at the time.

On the way to room temperature superconductivity, metallic hydrogen was proposed in 1968 [7] as a potential high-temperature superconductor

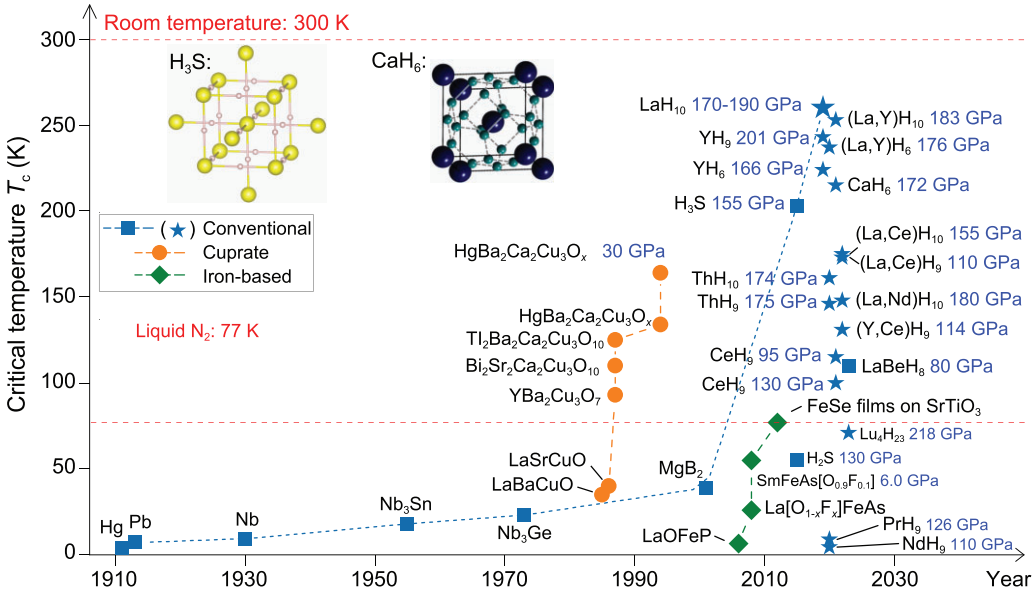

Figure 1. Chronological evolution of the superconducting critical temperature (T_c) for various superconductors. The square, circle and rhombus color blocks represent conventional, cuprate and iron-based superconductors, respectively. In particular, blue stars represent the conventional clathrate metal superhydride superconductors. The pressures required to synthesize these superconductors are represented by blue labels. Inset: crystal structures of covalently bonded hydrogen sulfide superconductor H_3S [22] (left panel) and clathrate superhydride CaH_6 [24] (right panel). The yellow, pink, black and green spheres represent the S, H, Ca and H atoms, respectively.

according to an equation within the superconductive picture of Bardeen-Cooper-Schrieffer (BCS) theory [8] showing that

$$T_c = 1.14\Theta_D \exp\left[-\frac{1}{N(0)V}\right], \qquad (1)$$

where Θ_D is the Debye temperature, $N(0)$ is the electron density of states at the Fermi energy and V is an effective pairing potential dominated by the attractive electron-phonon coupling interaction. Hydrogen, the most abundant element in the universe having the lightest atomic mass, naturally provides the highest possible Θ_D and V parameters for the solids that are necessary for a high-temperature phonon-mediated superconductivity.

At ambient pressure, solid hydrogen is a wide-gap insulator. It has been suggested that metallization of solid hydrogen would require a strong compression above a pressure of 500 GPa [9–12]. This raises a highly experimental challenge, especially when one deals with hydrogen, the number one element showing the most mobile behavior due to the smallest atomic core among the periodic table of elements. As a result, hydrogen atoms often go into the inside of diamond for a breakdown of the diamond anvil cell, a device for generation of high pressure. As a result, metallic hydrogen has not yet been obtained through a direct compression of solid hydrogen in experiments despite great efforts in the high-pressure research field [13,14].

As an alternative route, hydrogen-containing materials or hydrides play an important role in the pursuit of metallic hydrogen, and its high-temperature superconductivity. The idea was first proposed as early as 1971 [15] in a hypothetic system of Li–F–H and later in 2004 [16] in IV group hydrides (e.g. methane, silane and germane). It is believed that the introduction of non-hydrogen elements into the lattice inevitably causes a chemical pressure to be placed on hydrogen. The resultant metallization pressure of hydrides is significantly reduced compared to that needed for pure hydrogen. High-pressure experimental investigation of metallic hydrides in a lab becomes feasible at the current level of experimental technique.

In recent years, remarkable progress has been achieved in the discovery of high-temperature superconductors in superhydrides stabilized under high-pressure conditions with the established superconductivity T_c value approaching 260 K (−13 °C) for LaH_{10} [17–20], a record high T_c among known superconductors. Major findings are organized into two catalogues: (i) covalently bonded hydrogen sulfide superconductors (e.g. H_3S with T_c at ∼200 K) [21–23] and (ii) clathrate metal superhydride

superconductors (e.g. CaH_6 [24–26], YH_6 [17,27–30], YH_9 [17,28,30,31] and LaH_{10} [17–20] with $T_c = 215$, 220, 240 and 260 K, respectively), as represented by the blue stars in Fig. 1. Particular interest has been placed on the latter class of superconductors found in clathrate metal superhydrides that hold the record high superconductivity and have great potential to be those that superconduct at room temperature. In this peculiar class of clathrate superhydride superconductors, the first such example was theoretically proposed in a calcium superhydride CaH_6 back to 2012 [24], which was successfully synthesized in 2022 in a lab with a measured high T_c of 215 K under a pressure of 170 GPa [25,26].

In this article, we review recent progress on the findings of hydrogen-based high-temperature superconductors among superhydrides stabilized under high-pressure conditions, with a particular focus on the family of best-ever-known superconductors found in clathrate metal superhydrides. In the next two sections, we provide a brief overview of the discovery of covalently bonded hydrogen sulfide superconductors, and discuss the CALYPSO crystal structure prediction method and the role it plays in aiding the experimental discovery. Then in the following two sections we respectively discuss metal hydride superconductors at ambient pressure and at high pressures. The latter mainly focuses on clathrate superhydrides, and includes a discussion of the superconducting mechanism and the key features (e.g. structure motifs, bonding features, electronic structure, etc.) that govern the high superconductivity. In the final section, we discuss the future challenge and opportunity for room-temperature superconductors among clathrate metal superhydrides.

HYDROGEN SULFIDE SUPERCONDUCTORS AT A GLANCE

H_2S exists as a gas molecule in nature and smells of rotten eggs; it is the only stable stoichiometry compound found at ambient pressure in the hydrogen sulfide system. The work of Li *et al.* [21] is the original literature proposing sulfur hydride as a superconductor under high-pressure conditions.

Since 2014 when Li *et al.* made the first attempt to predict high-temperature superconductivity in sulfur dihydride [21], there has been much less interest in this system since it was believed to dissociate into its constituent elements of sulfur and hydrogen under pressure [32,33]. Li *et al.*'s extensive structure-searching simulation on hydrogen sulfide via the CALYPSO method [34,35] found that earlier proposed elemental dissociation would not occur, and a structure with a high superconductive potential consisting of $2(SH_3)$ units was predicted for H_2S with a theoretical T_c reaching 80 K at a pressure of 160 GPa [21].

This theoretical work [21] initiated the practical work by Eremets' group [23] where H_2S compressed in a diamond anvil cell was found to exhibit two astonishing superconductive states: (i) the one prepared at low temperature has a T_c of 30–150 K, in high accordance with the predicted H_2S superconductor [21]; (ii) the one annealed at room temperature exhibits an unexpected high T_c at 180–203 K, surpassing the earlier T_c record of 164 K [5] set by cuprate. The latter one has been ascribed to be H_3S through a stoichiometric change via a decomposition of H_2S into H_3S+S [36], where H_3S is a known stoichiometry of $(H_2S)_2H_2$ that has already been synthesized at a pressure of 7 GPa [37] and was later theoretically predicted to be a 200-K superconductor with a cubic structure (space group $Im\bar{3}m$) at megabar pressures [22]. In this cubic structure, each pair of S atoms symmetrically accommodates an atomic H between them, forming robust six-fold polar covalent S–H bonds (as shown in the inset of Fig. 1). The observed superconductivity in H_3S shows a strong isotopic effect pointing toward a phonon-mediated pairing mechanism [23].

The findings of hydrogen sulfide superconductors at a megabar pressure condition mark a milestone in superconductivity history and are a result of joint theoretical and experimental efforts, where theory plays a critical role in guiding the experimental exploration.

CALYPSO CRYSTAL STRUCTURE PREDICTION METHOD AND ITS ROLE IN AIDING EXPERIMENTAL DISCOVERY

Research on unknown superhydrides presents a challenge, as they can only be produced under megabar pressure conditions where limited information is available regarding their compositions and crystal structures. Moreover, owing to the weak X-ray scattering of hydrogen, the exact position of hydrogen is hardly determined by X-ray diffraction experiments. All these difficulties call for advanced theory that can predict the crystal structures of superhydrides in a reliable manner with only the chemical composition given. Recently developed theoretical crystal structure prediction methods [38,39] have taken center stage for this purpose, due to their trustworthy predictive power regarding compositions and structures. Over the years, techniques such as random search, genetic algorithm and swarm intelligence methods have evolved to become the

preferred choices for computational discovery of structures [38,39].

One may recall that crystal structure prediction presents a challenging, NP-hard problem in the minimization of the high-dimensional potential-energy surface (PES). To deal with this challenging problem, the CALYPSO (crystal structural analysis by particle swarm optimization) structure prediction method has been developed by the Ma group [34]. The method adopts a heuristic numerical solution scheme that is an optimal compromise between global exploration and local exploitation of the potential energy surface, making it particularly suited for crystal structure prediction. A number of algorithms has been devised in the method: (i) a symmetry classification searching strategy for high-coverage sampling of the potential energy surface; (ii) a bond characterization matrix for fingerprinting the structures and dividing the entire PES into a set of simpler fragments that are easier to explore and, most importantly, (iii) a swarm intelligence algorithm for rapid location of the energetically most stable structure by swarm-directed smart learning of optimal structures. The CALYPSO method has been coded into the same-name software [35] that is freely available for academic users, and it has proven a highly efficient and accurate tool for crystal structure prediction.

Given chemical compositions, CALYPSO can predict structures, in an intelligent and automatic way, for two- or three-dimensional crystals, nanoclusters and nanoparticles, protein molecules, reconstructed surfaces and interfaces, etc. The proof of the method's generality and reliability is in its utilization: up to now (June 2023), CALYPSO has been widely used in the world by more than 4000 researchers from 74 countries. Use of CALYPSO has generated many groundbreaking discoveries dedicated to high-pressure science, including the long-puzzled *o*C40 phase structure of semiconducting lithium, chemical compounds of Fe/Ni_3Xe, the substitutional alloy structure of Bi_2Te_3, the atomic structure of solid oxygen, counterintuitive compounds of H_3O and Ca_3O, the polymeric N_{10} structure, the superhard cubic phase of BC_3, etc. [39].

CALYPSO has played an important role in the design of hydrogen-based superconductors under high-pressure conditions. Besides the above-mentioned prediction of metallic and superconducting structures of H_2S [21], CALYPSO has been used to make breakthrough predictions on a class of clathrate metal superhydride superconductors (e.g. CaH_6 [24], YH_6 [27], YH_9 [17], LaH_{10} [17,18], etc.) that have received subsequent experimental confirmation. With the development of the crystal-structure searching methods, future design of room-temperature superhydride superconductors becomes feasible.

METAL HYDRIDE SUPERCONDUCTORS AT AMBIENT PRESSURE

The first hydride superconductor ever reported in 1970 was Th_4H_{15} with a T_c of 8 K at ambient pressure [40]. Later on, other binary metal hydride superconductors of PdH [41] and $NbH_{0.69}$ [42] were also reported with T_c values of ∼10 K. Several ternary metal hydride superconductors (e.g. HfV_2H [43] and $Pd_{0.55}Cu_{0.45}H_{0.7}$ [44] with T_c values of 4.8 and 16.6 K, respectively) were also synthesized.

It is worth noting that all these ambient-pressure metal hydride superconductors possess low superconductivity (<16.6 K). The top panel of Fig. 2 lists the most hydrogen-rich hydrides achieved at ambient pressure. It is seen that H contents in these ambient-pressure metal hydrides are generally low with a metal/H ratio larger than 1/3. In the crystal structures (Fig. 3), H atoms typically occupy the interstitial octahedral (O) or tetrahedral (T) sites of the closely packed metal lattice. In order to understand the physical origin for the low superconductivity at ambient pressure, the electron density of states of PdH [41], ScH_2 [45] and ScH_3 [45] are calculated, as shown in Fig. 3. It is found that hydrogen electrons are localized at a low-lying energy level, and do not contribute to the Fermi level. As a result, hydrogens in these low-H-content hydrides are not expected to play an important role in the superconductivity. It is worth noting that two properties of metal hydrides are crucial to achieving H-dominated high-T_c superconductivity: a large H-derived density of state at the Fermi level and large modifications of the electronic structure in response to the motions of H atoms (electron-phonon coupling) [17,38]. It is apparent that these ambient-pressure metal hydrides are not good candidates for the H-dominated superconductors.

From a chemical point of view, it is not unexpected to see such a negligible hydrogen electron contribution to the Fermi level in these hydrides. Metal hydrides can be regarded as M^+ cation-doped solid hydrogen (H_2). Once there is a formation of hydrides, valence electrons of metal atoms will transfer to H_2 molecules in the solid due to the large difference in electronegativities of hydrogen and metal atoms. The resultant electron occupancy of the antibonding σ^*_{1s} orbitals of H_2 molecules (Fig. 4) will lead to the dissociation of molecules into hydrogen atoms forming ionic $Pd^+ \ldots H^-$, $Sc_2^+ \ldots 2H^-$ and $Sc_3^+ \ldots 3H^-$ bonding states in PdH, ScH_2 and ScH_3,

Figure 2. Periodic table of experimental binary hydrides synthesized under ambient pressure (1 *atm.*, top panel) or high-pressure conditions (bottom panel). We use boxes with and without a black border to respectively distinguish between metal elements and covalent elements. Only the most hydrogen-rich species or those with the highest T_c (measured T_c values are preferred to the estimated ones) are listed, with theoretical predictions given a blue background and experimental results given an orange background. The related data were collected from Table 1, the Inorganic Crystal Structure Database [46] and other excellent reviews [47–49].

respectively. As a result, hydrogen electrons are confined in H^- states at deep energy levels far away from the Fermi level (Fig. 3).

Recently, a ternary N-doped lutetium hydride [50] was claimed to exhibit a remarkably high T_c of 294 K (21 °C) at a near-ambient pressure of 1 GPa. However, a number of subsequent experiments [51–53] that were able to reproduce the as-synthetic ternary product of N-doped lutetium hydride found no superconductivity at all for such a sample. From the current results achieved, it is suggested that such a claimed high superconductivity in an N-doped lutetium hydride is unlikely to be true.

CLATHRATE METAL SUPERHYDRIDE SUPERCONDUCTORS AT HIGH PRESSURES

Pressure as a thermodynamical variable can profoundly modify electronic orbitals and bonding patterns of hydrogen and metal atoms. It is thus a

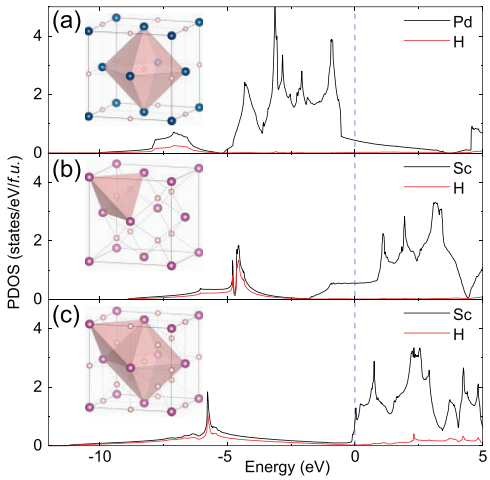

Figure 3. Crystal structures (inset) and partial electron density of states (PDOS) of *face-centered-cubic*-structured (a) PdH, (b) ScH_2 and (c) ScH_3 at ambient pressure. The blue, purple and pink spheres represent Pd, Sc and H atoms, respectively. Most H atoms occupy the interstitial octahedral (*O*) or tetrahedral (*T*) sites of the metal lattice. Solid black and red lines represent PDOS of metal and H, respectively. Blue dotted lines represent Fermi levels.

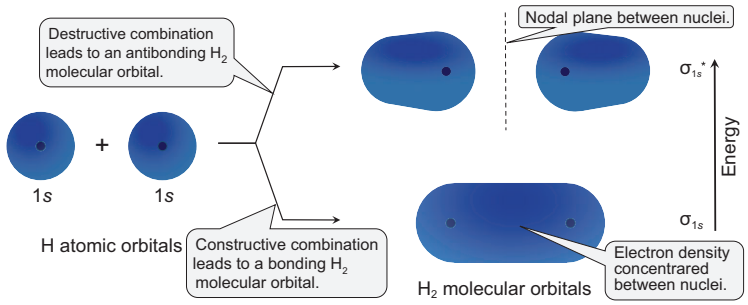

Figure 4. The formation of H_2 molecular orbitals from two H atomic orbitals based on molecular orbital theory, where the lower- (higher-)energy molecular orbital σ_{1s} (σ_{1s}^*) corresponds to the bonding (antibonding) behavior with electron density concentrated between (behind) the H nuclei.

powerful tool for the creation of exotic metal superhydrides (Fig. 2) that are not accessible at ambient conditions. As can be seen from Fig. 2, many new binary superhydrides appear with extremely high H content under high-pressure conditions. This opens a research avenue for finding high-temperature superconductors in these newly formed superhydrides.

A large number of superhydrides have been experimentally synthesized, some of which have been confirmed to be high-T_c superconductors, as listed in Table 1. Among various superhydrides, clathrate metal superhydrides take center stage since they exhibit the highest-T_c values (up to 250–260 K) known thus far.

CaH_6: the first clathrate superhydride

At ambient pressure, the only thermodynamically stable compound in the Ca–H system has a stoichiometry of CaH_2 that adopts a cotunnite-type structure and is not a superconductor (we refer the reader to our discussion on ambient-pressure hydrides). In 2012, through a structure search study on a mixture of Ca + H_2 using the CALYPSO method [34,35], we theoretically explored other calcium hydrides with higher hydrogen contents that can be stabilized under high-pressure conditions [24]. It was predicted that, besides CaH_2, three new stoichiometric calcium hydrides appear (Fig. 5(b)), CaH_4, CaH_6 and CaH_{12}, that are thermodynamically stable at the megabar pressure regime.

CaH_4 is not a superconductor and has a tetragonal *I*4/*mmm* structure (Fig. 5(b)) where Ca adopts a body-centered arrangement and H takes a mixed chemical form of monoatomic H and molecular H_2 [24]. Following our prediction, this proposed CaH_4 has been subsequently synthesized by two independent experimental works [55,56]. CaH_{12} has a rhombohedral structure consisting entirely of molecular H_2 units (Fig. 5(b)) that is not a good candidate for high-T_c superconductors [24].

Of particular interest is the prediction of a peculiar clathrate-structured CaH_6 that adopts a body-centered cubic structure (space group $Im\bar{3}m$; Figs 5(b) and 6(a)) where 24 H atoms form a perfect cage (eight hexagons plus six squares) with Ca at the center of the cage [24]. Within the H cage, there is clear charge localization (Fig. 6(b)) between nearest-neighboring H atoms and analysis of the electron localization function indicates that there is a weak covalent interaction between H atoms. It is interesting to note that all the nearest H–H distances are equal to 1.24 Å at 150 GPa. From the calculated partial electron density of states (Fig. 6(c)), we see that H electrons dominate the density of states at the Fermi level in this structure. As we have discussed in the above context, the dominant contribution of H electrons to the Fermi level is the most significant signature for the H-based superconductor. Here, CaH_6 must be the one that we really want in the hunt of a H-based high-T_c superconductor. Indeed, a realistic electron-phonon coupling calculation on CaH_6 gave a predicted exceptionally high T_c of 220 K at 150 GPa [24]. As expected, the H cage is found to be crucial to the superconductivity since it contributes most (84%) to the electron-phonon coupling parameter (Fig. 6(d)).

Although CaH_6 is the first-ever clathrate-type superhydride superconductor proposed in the field, its experimental synthesis has been regarded as one of the most challenging tasks. Previous attempts [55,56] on the synthesis use a mixture of Ca + H_2 or

Table 1. Measured superconducting transition temperature values (T_c in kelvins) of experimentally confirmed hydrides under ambient pressure and high-pressure conditions (P in gigapascals).

Class	Compound	P (GPa)	T_c (K)	Ref.
Hydride at 1 *atm.*	Th_4H_{15}	0	8.35	[40]
	PdH	0	9	[41]
	$Pd_{0.55}Cu_{0.45}H_{0.7}$	0	16.6	[44]
	HfV_2H	0	4.8	[43]
	$NbH_{0.69}$	0	9.4	[42]
Covalent hydride	SiH_4?	96	17	[72]
	H_2S	130	55	[23]
	H_3S	155	203	[23,73]
	H_3P?	207	103	[74]
Ionic hydride	$BaReH_9$	91	7	[75]
	Li_5MoH_{11}	160	6.5	[76]
	PtH	30	6.7	[77]
	ScH_3	131	18.5	[78]
	ZrH_3	9	11.6	[79,80]
	LuH_3	122	12.4	[78]
	TaH_3	197	30	[81]
	Zr_4H_{15}	40	4	[79]
	Hf_4H_{15}	23	4.5	[80]
Quasi-H_2-contained hydride	YH_4	155	88	[30,82]
	SnH_4	180	72	[83]
	$(La,Y)H_4$	111	92	[84]
	ZrH_6	220	71	[85]
	YH_7	162	29	[30]
	CeH_9	88	57	[86]
	SnH_{12}	200	70	[87]
	BaH_{12}	140	20	[88]
	HfH14	243	83	[89]
CaH_6-type clathrate	CaH_6	172	215	[25,26]
	YH_6	166	224	[28–30]
	EuH_6	152	–	[66]
	$(La,Y)H_6$	176	237	[71]
YH_9-type clathrate	YH_9	201	243	[28,30,31]
	CeH_9	130	100	[86]
	PrH_9	126	<9	[90]
	NdH_9	110	4.5	[91]
	EuH_9	170	–	[66]
	ThH_9	170	146	[92]
	$(Y,Ce)H_9$	114	131	[93]
	$(La,Ce)H_9$	100	176	[94]
LaH_{10}-type clathrate	LaH_{10}	188	260	[19,20]
	CeH_{10}	95	115	[86]
	ThH_{10}	174	161	[92]
	$(La,Y)H_{10}$	183	253	[71]
	$(La,Ce)H_{10}$	155	175	[95]
	$(La,Nd)H_{10}$	180	148	[96]
Ba_8Si_{46}-type clathrate	Ba_8H_{46}	27	–	[97]
	Eu_8H_{46}	86	–	[98]
	La_4H_{23}	96	–	[99]
	Lu_4H_{23}?	218	71	[100]
$LaBH_8$-type hydride	$LaBeH_8$	80	110	[101]

$CaH_2 + H_2$ as precursors. Unfortunately, this synthetic route leads to the easy formation of low-H content CaH_4 at a low-pressure region and further formation of high-H CaH_6 at the higher-pressure regime is kinetically hindered. Thanks to the concept of using ammonia borane [57–59] as the hydrogen source where it decomposes into boron mononitride and hydrogen at high-temperature conditions, one can control the hydride synthesis at a desirable pressure condition. Very recently, after 10 years of continuous effort, two independent experimental works [25,26] reported the successful syntheses of as-predicted clathrate-structured CaH_6 by using a mixture of Ca and ammonia borane as precursors. Experimentally measured T_c values for CaH_6 are 215 K at 172 GPa [25] and 210 K at 160 GPa [26], respectively.

Since we have various calcium hydrides at hand, it is possible to derive a general picture of the evolution of the chemical bonding of hydrogen to understand the formation mechanism of various calcium hydrides under pressure, as depicted in Fig. 5(b). Ca was introduced into solid molecular hydrogen as a dopant to achieve metallic hydrogen. As a result, there will be inevitable charge transfer from Ca into H_2 molecules. The accepted electrons by each H_2 molecule will occupy the antibonding σ^*_{1s} orbital (Fig. 4) since each H_2 molecule already has a filled σ_{1s} bond. The occupancy of this σ^*_{1s} orbital will lead to a weakening of the H–H bond, which in turn lengthens the H–H bond length and ultimately results in the complete dissociation of the H_2 molecule. The existence of monatomic H and H_2 units in the structures is contingent on the number of electrons each H_2 molecule accepts. If we assume that the two valence electrons of each Ca atom are fully 'ionized' and taken up by H_2 molecules, then the accepted electrons per H_2 for CaH_{12}, CaH_6, CaH_4 and CaH_2 are $\frac{1}{3}e$, $\frac{2}{3}e$, $1e$ and $2e$, respectively.

As for CaH_{12}, each H_2 molecule accepts $\frac{1}{3}e$ without severing the bond, but rather results in a bond elongation from 0.74 to 0.8–1.0 Å. In CaH_6, acceptance of $\frac{2}{3}e$ per H_2 molecule leads to the formation of the clathrate structure [24], where the H–H distance is in the range 1.0–1.3 Å and H–H is weakly covalently bonded. In CaH_4, there are two H_2 formulas in each unit cell and each H_2 molecule accepts $1e$. Given that two H_2 molecules are preserved, the remaining two H_2 molecules accommodate four 'excess' electrons into their σ^*_{1s} orbital. This process disrupts the molecules into monatomic hydrogen, with the H–H distances in the range 1.3–1.6 Å. In CaH_2, each H_2 molecule accepts $2e$. As a result, H_2 molecules dissociate fully into monatomic H.

We point out that H–H bonding features in calcium hydrides discovered under high-pressure

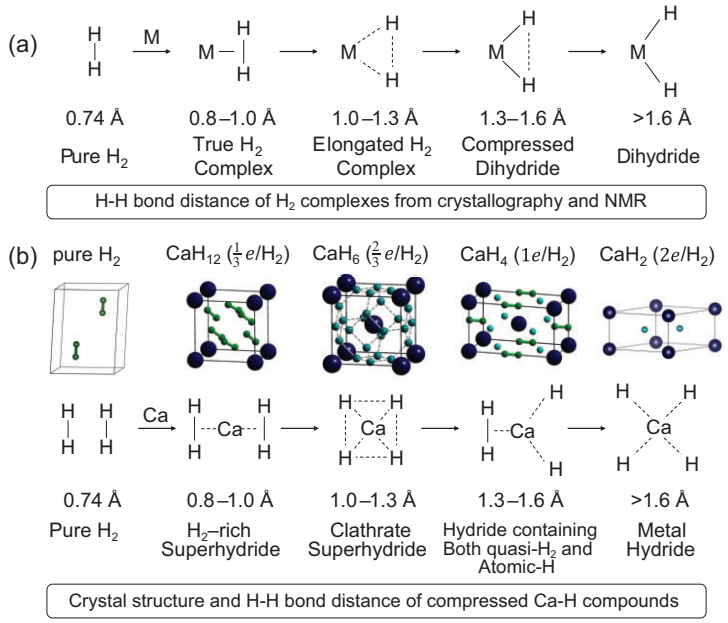

Figure 5. (a) The entire reaction coordinate for the activation of H_2 on a metal as a function of the degree of backdonation within the large regime of hundreds of LnM-H_2 complexes, Adapted with permission from [54]. Copyright 2007 American Chemical Society. (b) Several typical H-motifs of compressed metal. The corresponding crystal structures are illustrated with a Ca–H system as an example. H–H bond distance ($d_{H\text{-}H}$) of H_2 complexes (from crystallography and NMR) or H-motifs varying from 0.74 to >1.6 Å are shown.

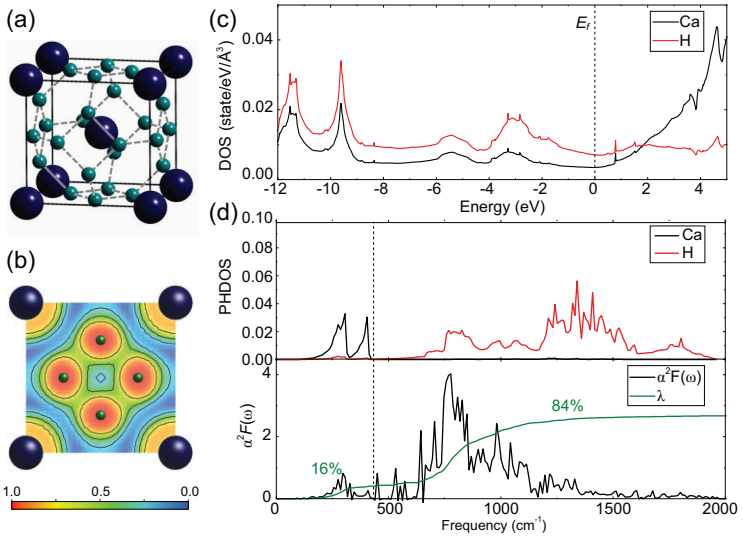

Figure 6. (a) Crystal structure, (b) the electron localization function, (c) the partial electron density of states and (d) projected phonon densities of states as well as the isotropic Eliashberg spectral function $\alpha^2F(\omega)$ and EPC parameter $\lambda(\omega)$ of CaH_6 at 150 GPa [24]. The small and large spheres in (a, b) represent H and Ca atoms, respectively.

conditions show excellent agreement with those in metal-inclusion H_2 complexes (LnM-H_2) at ambient pressure [54] (Fig. 5(a)) that have been well established by nuclear magnetic resonance experiments, as depicted in Fig. 5(a). This analogue for H–H bonding behaviors between calcium superhydrides stabilized under high-pressure conditions and H_2 complexes at ambient pressure is not accidental, but it rather reflects the true physics of hydrogen. We further emphasize that the current analysis of hydrogen bonding is also applied to the understanding of chemical bonding in other superhydrides and it is thus not necessary to discuss again in the context below to avoid any repetition.

Other CaH_6-type clathrate superhydrides

As a follow up to the theoretical proposal of clathrate CaH_6 as a high-temperature superconductor [24], other CaH_6-type clathrate superhydrides have also been predicted under high-pressure conditions, including, e.g. MgH_6[60], YH_6[17,27], ScH_6[17,61,62], PuH_6[63], TbH_6[64], EuH_6[65,66] and $(Yb/Lu)H_6$[67,68]. Among these, YH_6[17,27] has been experimentally synthesized under high-pressure conditions[28–30] with measured T_c values of up to 224 K at 166 GPa. These experimental works directly confirmed the theoretical prediction [17,27] of the clathrate structure and the high superconductivity above 200 K of YH_6. A strongly correlated system of clathrate EuH_6 has also been synthesized [66]; however, its superconductivity is absent due to the existence of magnetic properties in the system.

Several CaH_6-type alloyed clathrate superhydrides in ternary systems have been proposed by using the idea of partial substitution of Ca in CaH_6 or Y in YH_6 with alternative metal elements, e.g. $CaYH_{12}$ [69] and $YMgH_{12}$ superhydrides [70]. It is worth noting that a ternary clathrate alloyed $(La,Y)H_6$ superconductor has been experimentally synthesized with a measured T_c of 237 K at a pressure of 176 GPa [71].

YH_9-type clathrate superhydrides

In 2017, Peng *et al.* [17] theoretically proposed that clathrate structures are commonly formed in rare-earth superhydrides with stoichiometries besides CaH_6, with even higher hydrogen contents (e.g. YH_9 and LaH_{10}). The structure of YH_9 [17] in space group $P6_3/mmc$ can be regarded as a variant of CaH_6, although the number of hydrogen atoms in the hydrogen cage has been enlarged from 24 atoms in CaH_6 to 29 atoms in YH_9. In this H_{29} cage (Fig. 7(b)) where one Y atom sits at the center of the cage, there are six quadrilaterals, six pentagons and six regular hexagons [17]. YH_9 was computed to exhibit superconductivity with T_c reaching room temperature at 269 K at a pressure of 150 GPa. Soon after this theoretical prediction, two inde-

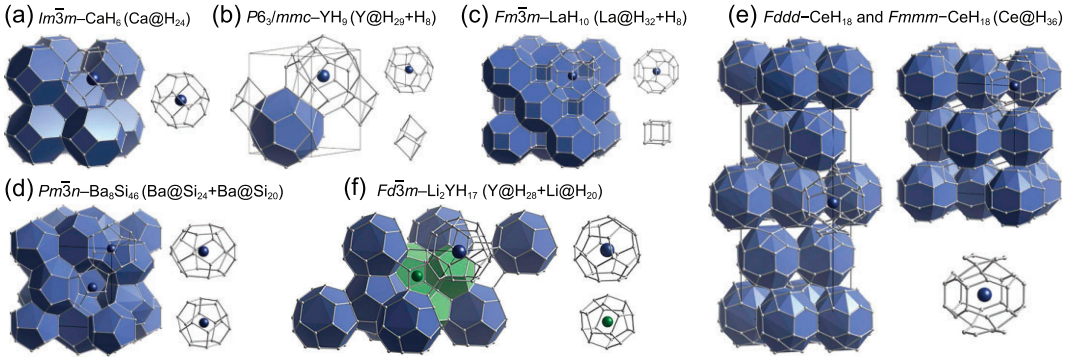

Figure 7. Crystal structures of several typical clathrate superhydrides and their H-motifs. (a) $Im\bar{3}m$–CaH_6, which is composed of Ca-centered H_{24} cages. (b) $P6_3/mmc$–YH_9, which is composed of Y-centered H_{29} cages and distorted H_8 cubes. (c) $Fm\bar{3}m$–LaH_{10}, which is composed of La-centered H_{32} cages and H_8 cubes. (d) Ba_8Si_{46}-type $Pm\bar{3}n$–Ba_8H_{46}, which is composed of Ba-centered H_{24} and Ba-centered H_{20} cages. (e) *Fddd*– and *Fmmm*–CeH_{18}, which are composed of Ce-centered H_{36} cages. (f) $Fd\bar{3}m$–Li_2YH_{17}, which is composed of Y-centered H_{28} and Li-centered H_{20} cages. The small and large spheres represent H and metal atoms, respectively.

pendent experiments successfully synthesized the clathrate-structured YH_9 and reported measured T_c values of 262 K at 182 GPa[31] and 243 K at 201 GPa[28].

Subsequent experimental efforts further successfully synthesized other YH_9-type rare-earth clathrate superhydrides in CeH_9[86], PrH_9[90], NdH_9[91] and EuH_9[66] with the measured highest T_c reaching 100 K for CeH_9[86]. These experimental results gave direct confirmation of theoretical predictions by Peng *et al.* [17]. A YH_9-type clathrate superhydride has also been reported in ThH_9 among actinide hydrides with the measured T_c reaching 146 K at a pressure of 170 GPa[92].

Recently, two YH_9-type ternary alloyed superhydrides of $(La,Ce)H_9$[94] and $(Y,Ce)H_9$[93] have been synthesized via random substitution of half Ce by La and Y, respectively. These two works demonstrated that substitutional alloying could act as an effective tool for substantially enhancing superconductivity since giant T_c enhancements are evidential. Superconductivity of 100 K in parent CeH_9 has been enhanced to 178 and 131 K in resultant child $(La,Ce)H_9$ and $(Y,Ce)H_9$, respectively, after substitutional alloying.

It is worth noting that the notably low synthesis pressures of 100–130 GPa for CeH_9, $(La,Ce)H_9$ and $(Y,Ce)H_9$ are believed to result from the particularly strong chemical pressure exerted by the delocalized 4*f* electrons of Ce. This suggests that other rare-earth hydrides with a similar delocalized *f* character may also be stable at relatively low pressures[102].

LaH_{10}-type clathrate superhydrides

In the same work for the proposal of YH_9-type superhydrides, Peng *et al.* [17] also theoretically proposed a class of clathrate rare-earth superhydrides in a stoichiometry of LaH_{10} with predicted T_c values as high as 288 K for LaH_{10} at 200 GPa and 303 K for YH_{10} at 400 GPa. The structure of LaH_{10} in space group $Fm\bar{3}m$ can also be regarded as a variant of the CaH_6-type structure, where the number of hydrogen atoms in the hydrogen cage has been enlarged from 24 atoms in CaH_6 to 32 atoms in LaH_{10}. The H_{32} cage (Fig. 7(c)) is composed of six squares and 12 regular hexagons [17]. Meanwhile, Liu *et al.* also independently predicted the clathrate-structured LaH_{10} and YH_{10} by a systematic exploration of the structures and superconductivities of La–H and Y–H systems under high-pressure conditions [18]. The as-predicted LaH_{10} has been successfully synthesized in two independent experiments [19,20] with measured T_c values of 250–260 K at pressures of 170–185 GPa.

The successful synthesis of LaH_{10} at pressures $<$200 GPa corroborated recent theoretical calculations by taking quantum effects into account [103] where the classical *ab initio* calculations [17,18] predicted structural distortions in the LaH_{10} below $\sim$230 GPa. The inclusion of zero-point energy has a clear effect on the stabilization of the $Fm\bar{3}m$ phase at a pressure regime as low as 129 GPa [103].

It is worth mentioning that the synthesis of LaH_{10} created a T_c record of 250–260 K (Fig. 1) approaching room temperature and ignited the hope of finding of room-temperature superconductivity in clathrate superhydrides. Subsequently, LaH_{10}-type clathrate superhydrides including CeH_{10} [86] and ThH_{10}[92] have also been experimentally synthesized with measured T_c values of 115 and 161 K, respectively. Substitutionally alloyed ternary LaH_{10}-type clathrate superhydrides in $(La,Y)H_{10}$[71], $(La,Ce)H_{10}$[95] and $(La,Nd)H_{10}$[96] have also

been experimentally synthesized with measured T_c values of 253, 175 and 148 K, respectively.

Ba_8Si_{46}-type clathrate superhydrides

It is known that clathrate structures often appear in a variety of silicon/germanium-based materials. Ba_8Si_{46} is one such good example, in the structure (Fig. 7(d)), and it is the first clathrate superconductor found in a bulk phase [104] with a measured T_c of 8 K at ambient pressure.

Several Ba_8Si_{46}-type clathrate superhydrides including Ba_8H_{46} [97], Eu_8H_{46} [98], La_4H_{23}[99] and Lu_4H_{23}[100] have been experimentally synthesized, among which Lu_4H_{23} has an observed T_c value up to 71 K at 218 GPa. No superconducting properties were experimentally studied for La_4H_{23} and Ba_8H_{46}, although they are expected to be high-T_c superconductors. Eu_8H_{46} is not a superconductor since it was predicted to exhibit a ferromagnetic property caused by the local unpaired *f* electrons of the Eu atom.

The theoretical proposal for thermodynamically stable Ca_8H_{46} and Sr_8H_{46} [105] is interesting; their predicted T_c at 200 GPa are 214 and 203 K, respectively. In addition, by performing a combination of high throughput screening and structural search, An *et al.* [106] predicted a thermodynamically stable Ba_8Si_{46}-type superhydride of $LiNa_3H_{23}$ that exhibits an extraordinarily high T_c of 310 K at 350 GPa.

CeH_{18}-type clathrate superhydrides

Very recently, a new class of extremely hydrogen-rich CeH_{18}-type clathrate superhydrides with a stoichiometry of CeH_{18} were theoretically proposed in rare-earth/actinide superhydrides [107]. These peculiar superhydrides are composed of H_{36} cages (Fig. 7(e)), the largest cage for a known clathrate superhydride structure. This CeH_{18}-type clathrate superhydride forms a crystal structure with either the *Fddd* or *Fmmm* space group. In this structure, H_{36} cages are interconnected by a $6H_6$ ribbon-ring structure. Two undulating H_6 hexagons are positioned above and below this structure, with bridge bonds linking the H_6 hexagons to the $6H_6$ ribbon ring (as shown in Fig. 7(e)). First-principles calculations [107] for different CeH_{18}-type clathrate superhydrides predict diverse T_c values among the same stoichiometry. Among these extreme superhydrides, CeH_{18} and ThH_{18} are particularly noteworthy. They display superconductivity above room temperature, with T_c values peaking at 330 K at 350 GPa and 321 K at 600 GPa, respectively. These represent the highest predicted T_c values among all known thermodynamically stable superhydrides. Future experiments are highly desirable for the synthesis of this class of CeH_{18}-type clathrate superhydrides to search for room-temperature superconductors.

Ternary clathrate superhydrides

Binary superhydrides have been exhaustively investigated both theoretically and experimentally [47]. The quest for high-T_c superconductors among superhydrides has recently evolved, moving beyond the realm of binary compounds and shifting focus towards ternary ones, which offer a vast array of material types and configurations. Ternary superhydrides can enjoy advantageous properties through tuning of two non-hydrogen elements in structures, leading to superior superconducting properties beyond those of binary hydrides. Earlier theoretical works [108,109] have revealed promising ternary superhydrides that superconduct at or above room temperature. However, the challenge remains to attain stoichiometric ternary compounds with a well-resolved crystal structure that can host high-temperature superconductivity above 100 K. Although several examples of ternary substitutionally alloyed clathrate superhydrides (e.g. $(La,Ce)H_9$ and $(Y,Ce)H_9$) have been discussed in the aforementioned text where the primary focus is placed on enhancing superconductivity through elemental substitution on known binary clathrate hydride superconductors, these activities have not offered any new prototype ternary structure for high-temperature superconductivity.

On the way to finding room-temperature superconductors among ternary superhydrides, a significant research question in this field is how to stabilize a superhydride that incorporates as many hydrogen atoms as possible, without forming any H_2 molecules within the lattice, in order to achieve a hydrogen-dominated electron density of states at the Fermi surface [17,38]. A useful strategy is to introduce extra electrons via metal doping into H_2-rich binary superhydrides [110], as has been demonstrated in the design of clathrate-structured ternary Li_2MgH_{16}[110] and Li_2Y/LaH_{17}[111]. Li_2MgH_{16} has been predicted to exhibit 'hot' superconductivity with a T_c value of up to 473 K at 250 GPa, which is the highest predicted T_c among all known superhydride superconductors [110]. The Li_2Y/LaH_{17} clathrate structure comprises Li-centered H_{20} cages and Y/La-centered H_{28} cages, where each H_{20} or H_{28} cage consists of 12 pentagons or 12 pentagons and four hexagons (Fig. 7(f)). It is worth noting that the estimated T_c values of Li_2YH_{17} and Li_2LaH_{17} are relatively low with maximum values of 108 K at 200 GPa and 156 K at 160 GPa, respectively [111].

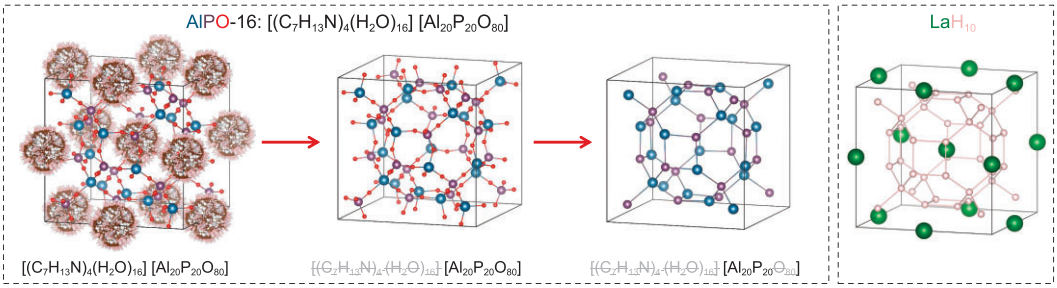

Figure 8. Comparison of the H sublattice in clathrate LaH_{10} and the AST-type zeolite framework in an $AlPO_4$-16 material.

The challenge of achieving room-temperature superconductivity at significantly lower pressures is a recognized issue. A strategy to address this challenge is to use small-radius elements (e.g. B or Be) and hydrogen to achieve ternary superhydride superconductors with alloy backbones [112]. By employing this approach, a range of $LaBH_8$-type ternary superhydrides with a 'fluorite-type' backbone have been proposed [112–114], among which $LaBeH_8$ [112] is anticipated to be a thermodynamically stable phase above 98 GPa and dynamically stable down to 20 GPa with a high T_c of 185 K. Very recently, $LaBeH_8$ has been successfully synthesized with a measured T_c of up to 110 K at 80 GPa [101]. $LaBeH_8$ is the first experimental realization of an archetype ternary prototype with exact stoichiometry, well-resolved structure and T_c beyond 100 K.

Clathrate frameworks at ambient pressure

Hydrogen clathrate structures in superhydrides stabilized under high-pressure conditions are a class of peculiar structures quipped for hydrogen-based superconductors. As we have discussed above, the clathrate structure is the key to create the observed high superconductivity in superhydrides that holds the record high-T_c values among superconductors known thus far. However, these hydrogen clathrate structures can only be stabilized at megabar pressures and are not capturable at ambient pressure upon the release of pressure. For any practical application, it is essential to discover superconductors at ambient pressure.

From a structure point of view, we find two kinds of analogous materials at ambient pressure: (i) CaH_6-, Ba_8H_{46}- and Li_2YH_{17}-type superhydrides are structurally equivalent to the type-VII, type-I and type-II silicon-based clathrate structures, respectively; (ii) hydrogen sublattices in CaH_6-, LaH_{10}-, Ba_8Si_{46}- and Li_2YH_{17}-type superhydrides share the structure similarity to the known SOD-, AST-, MEP- and MTN-type zeolite frameworks, respectively.

To understand how clathrate structures in superhydrides are related to zeolite frameworks, we take LaH_{10} [17,18] as an example for the illustration (Fig. 8) whose hydrogen sublattice shares the structure similarity with the AST-type zeolite framework in an aluminum phosphate $AlPO_4$-16 material [115]. It is noted that, when all non-framework cations are removed, $AlPO_4$-16 turns out to be an open three-dimensional framework structure composed of corner-sharing TO_4 (T = Al and P) tetrahedra (Fig. 8). The network of T atoms is identical to the hydrogen sublattice in LaH_{10}.

The structure similarity between clathrate superhydrides and silicon-based clathrate or zeolite materials may give a hint on future design of high-T_c superconductors at ambient pressure. Encouragingly, there exists a large number of clathrate materials at ambient pressure that might be useful as templates for such a design. For example, over 200 zeolite framework types of material have been documented [116].

CONCLUSION AND OUTLOOK

In this review, we provide an up-to-date perspective on the research field of superconducting clathrate superhydrides under high-pressure conditions. Clathrate superhydrides have emerged as the most promising candidates for hunting high-temperature superconductors. Finding room-temperature superconductors along this direction might become true in a near future.

Multi-element superhydrides are the immediate targets for the discovery of high-temperature superconductors. As the number of elements increase in hydrides, the number of conceivable structures and potential superconducting compounds grows rapidly [108,117], suggesting that there are more open rooms for clathrate superhydrides in ternary and quaternary systems than those in binary ones. However, the exponential growth of chemical space with increasing element species makes the search a great challenge both theoretically and experimentally. Therefore, it might be useful to summarize

several strategies to accelerate the design of high-temperature superconducting superhydrides based on successful experiences: (i) doping/substituting metal elements into known clathrate superhydrides; (ii) introducing extra electrons via metal doping into known superhydrides that contain abundant quasi-H_2 molecular units [110]; (iii) using small-radius elements to stabilize ternary hydrogen-based superconductors with alloy backbones [112]; (iv) atomic substitution of known clathrate materials at ambient pressure.

Given the rapid development of this field, we anticipate that certain aspects of this review might shortly become outdated. However, we trust that the methodological framework and the amalgamation of knowledge from both experiments and theories outlined here will provide a useful reference for future research and inspire exciting future discoveries.

FUNDING

This work was supported by the Major Program of the National Natural Science Foundation of China (52090024), the Strategic Priority Research Program of Chinese Academy of Sciences (XDB33000000) and the National Natural Science Foundation of China (12074138, 52288102, 12374009 and 12034009).

AUTHOR CONTRIBUTIONS

Y.M. conceived the project. Y.S. and Y.M. co-wrote the manuscript. All authors discussed the results, participated in analyzing the data and commented on the manuscript.

Conflict of interest statement. None declared.

REFERENCES

1. Onnes HK. The resistance of pure mercury at helium temperatures. *Commun Phys Lab Univ Leiden* 1911; **12**: 1.
2. Meissner W and Ochsenfeld R. Ein neuer effekt bei eintritt der supraleitfähigkeit. *Naturwissenschaften* 1933; **21**: 787–8.
3. Schilling A, Cantoni M and Guo JD *et al.* Superconductivity above 130 K in the Hg–Ba–Ca–Cu–O system. *Nature* 1993; **363**: 56–8.
4. Chu CW, Gao L and Chen F *et al.* Superconductivity above 150 K in $HgBa_2Ca_2Cu_3O_{8+\delta}$ at high pressures. *Nature* 1993; **365**: 323–5.
5. Gao L, Xue YY and Chen F *et al.* Superconductivity up to 164 K in $HgBa_2Ca_{m-1}Cu_mO_{2m+2+\delta}$ (m = 1, 2, and 3) under quasi-hydrostatic pressures. *Phys Rev B* 1994; **50**: 4260–3.
6. Ren ZA, Che GC and Dong XL *et al.* Superconductivity and phase diagram in iron-based arsenic-oxides $ReFeAsO_{1-\delta}$ (Re = rare-earth metal) without fluorine doping. *Europhys Lett* 2008; **83**: 17002.
7. Ashcroft NW. Metallic hydrogen: a high-temperature superconductor? *Phys Rev Lett* 1968; **21**: 1748.
8. Bardeen J, Cooper LN and Schrieffer JR. Microscopic theory of superconductivity. *Phys Rev* 1957; **106**: 162.
9. Pickard CJ and Needs RJ. Structure of phase III of solid hydrogen. *Nat Phys* 2007; **3**: 473–6.
10. Zhang L, Niu Y and Li Q *et al. Ab Initio* prediction of superconductivity in molecular metallic hydrogen under high pressure. *Solid State Commun* 2007; **141**: 610–4.
11. McMahon JM and Ceperley DM. Ground-state structures of atomic metallic hydrogen. *Phys Rev Lett* 2011; **106**: 165302.
12. Liu H, Wang H and Ma Y. Quasi-molecular and atomic phases of dense solid hydrogen. *J Phys Chem C* 2012; **116**: 9221–6.
13. Eremets MI, Drozdov AP and Kong PP *et al.* Semimetallic molecular hydrogen at pressure above 350 GPa. *Nat Phys* 2019; **15**: 1246–9.
14. Loubeyre P, Occelli F and Dumas P. Synchrotron infrared spectroscopic evidence of the probable transition to metal hydrogen. *Nature* 2020; **577**: 631–5.
15. Gilman JJ. Lithium dihydrogen fluoride—an approach to metallic hydrogen. *Phys Rev Lett* 1971; **26**: 546.
16. Ashcroft NW. Bridgman's high-pressure atomic destructibility and its growing legacy of ordered states. *J Phys: Condens Matter* 2004; **16**: S945–52.
17. Peng F, Sun Y and Pickard CJ *et al.* Hydrogen clathrate structures in rare earth hydrides at high pressures: possible route to room-temperature superconductivity. *Phys Rev Lett* 2017; **119**: 107001.
18. Liu H, Naumov II and Hoffmann R *et al.* Potential high-T_c superconducting lanthanum and yttrium hydrides at high pressure. *Proc Natl Acad Sci USA* 2017; **114**: 6990–5.
19. Drozdov AP, Kong PP and Minkov VS *et al.* Superconductivity at 250 K in lanthanum hydride under high pressures. *Nature* 2019; **569**: 528–31.
20. Somayazulu M, Ahart M and Mishra AK *et al.* Evidence for superconductivity above 260 K in lanthanum superhydride at megabar pressures. *Phys Rev Lett* 2019; **122**: 027001.
21. Li Y, Hao J and Liu H *et al.* The metallization and superconductivity of dense hydrogen sulfide. *J Chem Phys* 2014; **140**: 174712.
22. Duan D, Liu Y and Tian F *et al.* Pressure-induced metallization of dense $(H_2S)_2H_2$ with high-T_c superconductivity. *Sci Rep* 2014; **4**: 6968.
23. Drozdov AP, Eremets MI and Troyan IA *et al.* Conventional superconductivity at 203 kelvin at high pressures in the sulfur hydride system. *Nature* 2015; **525**: 73–6.
24. Wang H, Tse JS and Tanaka K *et al.* Superconductive sodalite-like clathrate calcium hydride at high pressures. *Proc Natl Acad Sci USA* 2012; **109**: 6463–6.
25. Ma L, Wang K and Xie Y *et al.* High-temperature superconducting phase in clathrate calcium hydride CaH_6 up to 215 K at a pressure of 172 GPa. *Phys Rev Lett* 2022; **128**: 167001.
26. Li Z, He X and Zhang C *et al.* Superconductivity above 200 K discovered in superhydrides of calcium. *Nat Commun* 2022; **13**: 2863.
27. Li Y, Hao J and Liu H *et al.* Pressure-stabilized superconductive yttrium hydrides. *Sci Rep* 2015; **5**: 9948.

28. Kong P, Minkov VS and Kuzovnikov MA *et al.* Superconductivity up to 243 K in the yttrium-hydrogen system under high pressure. *Nat Commun* 2021; **12**: 5075.
29. Troyan IA, Semenok DV and Kvashnin AG *et al.* Anomalous high-temperature superconductivity in YH_6. *Adv Mater* 2021; **33**: 2006832.
30. Wang Y, Wang K and Sun Y *et al.* Synthesis and superconductivity in yttrium superhydrides under high pressure. *Chinese Phys B* 2022; **31**: 106201.
31. Snider E, Dasenbrock-Gammon N and McBride R *et al.* Synthesis of yttrium superhydride superconductor with a transition temperature up to 262 K by catalytic hydrogenation at high pressures. *Phys Rev Lett* 2021; **126**: 117003.
32. Rousseau R, Boero M and Bernasconi M *et al. Ab initio* simulation of phase transitions and dissociation of H_2S at high pressure. *Phys Rev Lett* 2000; **85**: 1254.
33. Fujihisa H, Yamawaki H and Sakashita M *et al.* Molecular dissociation and two low-temperature high-pressure phases of H_2S. *Phys Rev B* 2004; **69**: 214102.
34. Wang Y, Lv J and Zhu L *et al.* Crystal structure prediction via particle-swarm optimization. *Phys Rev B* 2010; **82**: 094116.
35. Wang Y, Lv J and Zhu L *et al.* CALYPSO: a method for crystal structure prediction. *Comput Phys Commun* 2012; **183**: 2063–70.
36. Li YW, Wang L and Liu HY *et al.* Dissociation products and structures of solid H_2S at strong compression. *Phys Rev B* 2016; **93**: 020103.
37. Strobel TA, Ganesh P and Somayazulu M *et al.* Novel cooperative interactions and structural ordering in H_2S-H_2. *Phys Rev Lett* 2011; **107**: 255503.
38. Zhang L, Wang Y and Lv J *et al.* Materials discovery at high pressures. *Nat Rev Mater* 2017; **2**: 17005.
39. Wang Y, Lv J and Gao P *et al.* Crystal structure prediction via efficient sampling of the potential energy surface. *Acc Chem Res* 2022; **55**: 2068–76.
40. Satterthwaite CB and Toepke IL. Superconductivity of hydrides and deuterides of thorium. *Phys Rev Lett* 1970; **25**: 741.
41. Skośkiewicz T. Superconductivity in the palladium-hydrogen system. *Phys Stat Sol (b)* 1973; **59**: 329–34.
42. Welter JM and Johnen FJ. Superconducting transition temperature and low temperature resistivity in the niobium-hydrogen system. *Z Physik B* 1977; **27**: 227–32.
43. Duffer P, Gualtieri DM and Rao VUS. Pronounced isotope effect in the superconductivity of HfV_2 containing hydrogen (deuterium). *Phys Rev Lett* 1976; **37**: 1410.
44. Stritzker B. High superconducting transition temperatures in the palladium-noble metal-hydrogen system. *Z Physik* 1974; **268**: 261–4.
45. Economou EN. Superconductivity in palladium based hydrides. In: Bambakidis G (ed.) *Metal Hydrides*. Boston, MA: Springer, 1981, 1–19.
46. Bergerhoff G, Hundt R and Sievers R *et al.* The inorganic crystal structure data base. *J Chem Inf Comput Sci* 1983; **23**: 66–9.
47. Gao G, Wang L and Li M *et al.* Superconducting binary hydrides: theoretical predictions and experimental progresses. *Mater Today Phys* 2021; **21**: 100546.
48. Wang D, Ding Y and Mao HK. Future study of dense superconducting hydrides at high pressure. *Materials* 2021; **14**: 7563.
49. Du M, Zhao W and Cui T *et al.* Compressed superhydrides: the road to room temperature superconductivity. *J Phys: Condens Matter* 2022; **34**: 173001.
50. Dasenbrock-Gammon N, Snider E and McBride R *et al.* Evidence of near-ambient superconductivity in a N-doped lutetium hydride. *Nature* 2023; **615**: 244–50.
51. Peng D, Zeng Q and Lan F *et al.* The near-room-temperature upsurge of electrical resistivity in Lu-H-N is not superconductivity, but a metal-to-poor-conductor transition. *Matter Radiat Extremes* 2023; **8**: 058401.
52. Xing X, Wang C and Yu L *et al.* Observation of non-superconducting phase changes in nitrogen doped lutetium hydrides. *Nat Commun* 2023; **14**: 5991.
53. Ming X, Zhang YJ and Zhu X *et al.* Absence of near-ambient superconductivity in $LuH_{2\pm x}N_y$. *Nature* 2023; **620**: 72–7.
54. Kubas GJ. Fundamentals of H_2 binding and reactivity on transition metals underlying hydrogenase function and H_2 production and storage. *Chem Rev* 2007; **107**: 4152–205.
55. Mishra AK, Muramatsu T and Liu H *et al.* New calcium hydrides with mixed atomic and molecular hydrogen. *J Phys Chem C* 2018; **122**: 19370–8.
56. Wu G, Huang X and Xie H *et al.* Unexpected calcium polyhydride CaH_4: a possible route to dissociation of hydrogen molecules. *J Chem Phys* 2019; **150**: 044507.
57. Chellappa RS, Somayazulu M and Struzhkin VV *et al.* Pressure-induced complexation of NH_3BH_3–H_2. *J Chem Phys* 2009; **131**: 224515.
58. Song Y. New perspectives on potential hydrogen storage materials using high pressure. *Phys Chem Chem Phys* 2013; **15**: 14524–47.
59. Potter RG, Somayazulu M and Cody G *et al.* High pressure equilibria of dimethylamine borane, dihydridobis (dimethylamine) boron (III) tetrahydridoborate (III), and hydrogen. *J Phys Chem C* 2014; **118**: 7280–7.
60. Feng X, Zhang J and Gao G *et al.* Compressed sodalite-like MgH_6 as a potential high-temperature superconductor. *RSC Adv* 2015; **5**: 59292–6.
61. Abe K. Hydrogen-rich scandium compounds at high pressures. *Phys Rev B* 2017; **96**: 144108.
62. Ye X, Zarifi N and Zurek E *et al.* High hydrides of scandium under pressure: potential superconductors. *J Phys Chem C* 2018; **122**: 6298–309.
63. Zhao J, Ao B and Li S *et al.* Phase diagram and bonding states of Pu–H binary compounds at high pressures. *J Phys Chem C* 2020; **124**: 7361–9.
64. Hai YL, Lu N and Tian HL *et al.* Cage structure and near room-temperature superconductivity in TbH_n ($n = 1$–12). *J Phys Chem C* 2021; **125**: 3640–9.
65. Semenok DV, Kruglov IA and Savkin IA *et al.* On distribution of superconductivity in metal hydrides. *Curr Opin Solid State Mater Sci* 2020; **24**: 100808.
66. Ma L, Zhou M and Wang Y *et al.* Experimental clathrate superhydrides EuH_6 and EuH_9 at extreme pressure conditions. *Phys Rev Res* 2021; **3**: 043107.
67. Sun WG, Kuang XY and Keen HDJ *et al.* Second group of high-pressure high-temperature lanthanide polyhydride superconductors. *Phys Rev B* 2020; **102**: 144524.
68. Du M, Song H and Zhang Z *et al.* Room-temperature superconductivity in Yb/Lu substituted clathrate hexahydrides under moderate pressure. *Research* 2022; **2022**: 9784309.
69. Liang X, Bergara A and Wang L *et al.* Potential high-T_c superconductivity in $CaYH_{12}$ under pressure. *Phys Rev B* 2019; **99**: 100505.
70. Song P, Hou Z and de Castro PB *et al.* The systematic study on the stability and superconductivity of Y–Mg–H compounds under high pressure. *Adv Theory Simul* 2022; **5**: 2100364.
71. Semenok DV, Troyan IA and Ivanova AG *et al.* Superconductivity at 253 K in lanthanum–yttrium ternary hydrides. *Mater Today* 2021; **48**: 18–28.
72. Eremets MI, Trojan IA and Medvedev SA *et al.* Superconductivity in hydrogen dominant materials: silane. *Science* 2008; **319**: 1506–9.
73. Osmond I, Moulding O and Cross S *et al.* Clean-limit superconductivity in Im-3m–H_3S synthesized from sulfur and hydrogen donor ammonia borane. *Phys Rev B* 2022; **105**: L220502.
74. Drozdov AP, Eremets MI and Troyan IA. Superconductivity above 100 K in PH_3 at high pressures, arXiv, 1508.06224.
75. Muramatsu T, Wanene WK and Somayazulu M *et al.* Metallization and superconductivity in the hydrogen-rich ionic salt $BaReH_9$. *J Phys Chem C* 2015; **119**: 18007–13.

76. Meng D, Sakata M and Shimizu K *et al.* Superconductivity of the hydrogen-rich metal hydride Li_5MoH_{11} under high pressure. *Phys Rev B* 2019; **99**: 024508.
77. Matsuoka T, Hishida M and Kuno K *et al.* Superconductivity of platinum hydride. *Phys Rev B* 2019; **99**: 144511.
78. Shao M, Chen S and Chen W *et al.* Superconducting ScH_3 and LuH_3 at megabar pressures. *Inorg Chem* 2021; **60**: 15330–5.
79. Xie H, Zhang W and Duan D *et al.* Superconducting zirconium polyhydrides at moderate pressures. *J Phys Chem Lett* 2020; **11**: 646–51.
80. Kuzovnikov MA and Tkacz M. High-pressure synthesis of novel polyhydrides of of Zr and Hf with a Th_4H_{15}-type structure. *J Phys Chem C* 2019; **123**: 30059–66.
81. He X, Zhang CL and Li ZW *et al.* Superconductivity observed in tantalum polyhydride at high pressure. *Chin Phys Lett* 2023; **40**: 057404.
82. Shao M, Chen W and Zhang K *et al.* High-pressure synthesis of superconducting clathratelike YH_4. *Phys Rev B* 2021; **104**: 174509.
83. Troyan IA, Semenok DV and Ivanova AG *et al.* Non-Fermi-liquid behavior of superconducting SnH_4. *Adv Sci* 2023; **10**: 2303622.
84. Bi J, Nakamoto Y and Zhang P *et al.* Stabilization of superconductive La–Y alloy superhydride with T_c above 90 K at megabar pressure. *Mater Today Phys* 2022; **28**: 100840.
85. Zhang C, He X and Li Z *et al.* Superconductivity in zirconium polyhydrides with T_c above 70 K. *Sci Bull* 2022; **67**: 907–9.
86. Chen W, Semenok DV and Huang X *et al.* High-temperature superconducting phases in cerium superhydride with a T_c up to 115 K below a pressure of 1 megabar. *Phys Rev Lett* 2021; **127**: 117001.
87. Hong F, Shan P and Yang L *et al.* Possible superconductivity at ∼70 K in tin hydride SnH_x under high pressure. *Mater Today Phys* 2022; **22**: 100596.
88. Chen W, Semenok DV and Kvashnin AG *et al.* Synthesis of molecular metallic barium superhydride: pseudocubic BaH_{12}. *Nat Commun* 2021; **12**: 273.
89. Zhang CL, He X and Li ZW *et al.* Superconductivity above 80 K in polyhydrides of hafnium. *Mater Today Phys* 2022; **27**: 100826.
90. Zhou D, Semenok DV and Duan D *et al.* Superconducting praseodymium superhydrides. *Sci Adv* 2020; **6**: eaax6849.
91. Zhou D, Semenok DV and Xie H *et al.* High-pressure synthesis of magnetic neodymium polyhydrides. *J Am Chem Soc* 2020; **142**: 2803–11.
92. Semenok DV, Kvashnin AG and Ivanova AG *et al.* Superconductivity at 161 K in thorium hydride ThH_{10}: synthesis and properties. *Mater Today* 2020; **33**: 36–44.
93. Chen LC, Luo T and Dalladay-Simpson P *et al.* Synthesis and superconductivity in yttrium-cerium hydrides at moderate pressures, arXiv, 2208.05191.
94. Bi J, Nakamoto Y and Zhang P *et al.* Giant enhancement of superconducting critical temperature in substitutional alloy $(La,Ce)H_9$. *Nat Commun* 2022; **13**: 5952.
95. Huang G, Luo T and Dalladay-Simpson P *et al.* Synthesis of superconducting phase of $La_{0.5}Ce_{0.5}H_{10}$ at high pressures, arXiv, 2208.05199.
96. Semenok DV, Troyan IA and Sadakov AV *et al.* Effect of magnetic impurities on superconductivity in LaH_{10}. *Adv Mater* 2022; **34**: 2204038.
97. Pena-Alvarez M, Binns J and Martinez-Canales M *et al.* Synthesis of Weaire–Phelan barium polyhydride. *J Phys Chem Lett* 2021; **12**: 4910–6.
98. Semenok DV, Zhou D and Kvashnin AG *et al.* Novel strongly correlated europium superhydrides. *J Phys Chem Lett* 2020; **12**: 32–40.
99. Laniel D, Trybel F and Winkler B *et al.* High-pressure synthesis of seven lanthanum hydrides with a significant variability of hydrogen content. *Nat Commun* 2022; **13**: 6987.
100. Li Z, He X and Zhang C *et al.* Superconductivity above 70 K observed in lutetium polyhydrides. *Sci China-Phys Mech Astron* 2023; **66**: 267411.
101. Song Y, Bi J and Nakamoto Y *et al.* Stoichiometric ternary superhydride $LaBeH_8$ as a new template for high-temperature superconductivity at 110 K under 80 GPa. *Phys Rev Lett* 2023; **130**: 266001.
102. Jeon H, Wang C and Yi S *et al.* Origin of enhanced chemical precompression in cerium hydride CeH_9. *Sci Rep* 2020; **10**: 16878.
103. Errea I, Belli F and Monacelli L *et al.* Quantum crystal structure in the 250-kelvin superconducting lanthanum hydride. *Nature* 2020; **578**: 66–9.
104. Yamanaka S, Enishi E and Fukuoka H *et al.* High-pressure synthesis of a new silicon clathrate superconductor, Ba_8Si_{46}. *Inorg Chem* 2000; **39**: 56–8.
105. Sun Y and Miao M. Assemble superhydrides with non-integer h/metal ratios on metal templates, arXiv, 2303.05721.
106. An D, Duan D and Zhang Z *et al.* Thermodynamically stable room-temperature superconductors in Li–Na hydrides under high pressures, arXiv, 2303.09805.
107. Zhong X, Sun Y and Iitaka T *et al.* Prediction of above-room-temperature superconductivity in lanthanide/actinide extreme superhydrides. *J Am Chem Soc* 2022; **144**: 13394–400.
108. Flores-Livas JA, Boeri L and Sanna A *et al.* A perspective on conventional high-temperature superconductors at high pressure: methods and materials. *Phys. Rep.* 2020; **856**: 1–78.
109. Zhang XH, Zhao YP and Yang GC. Superconducting ternary hydrides under high pressure. *WIREs Comput Mol Sci* 2022; **12**: e1582.
110. Sun Y, Lv J and Xie Y *et al.* Route to a superconducting phase above room temperature in electron-doped hydride compounds under high pressure. *Phys Rev Lett* 2019; **123**: 097001.
111. Sun Y, Wang Y and Zhong X *et al.* High-temperature superconducting ternary Li–R–H superhydrides at high pressures (R = Sc, Y, La). *Phys Rev B* 2022; **106**: 024519.
112. Zhang Z, Cui T and Hutcheon MJ *et al.* Design principles for high-temperature superconductors with a hydrogen-based alloy backbone at moderate pressure. *Phys Rev Lett* 2022; **128**: 047001.
113. Di Cataldo S, Heil C and von der Linden W *et al.* $LaBH_8$: towards high-T_c low-pressure superconductivity in ternary superhydrides. *Phys Rev B* 2021; **104**: L020511.
114. Liang X, Bergara A and Wei X *et al.* Prediction of high-T_c superconductivity in ternary lanthanum borohydrides. *Phys Rev B* 2021; **104**: 134501.
115. Bennett JM and Kirchner RM. The structure of as-synthesized $AlPO_4$–16 determined by a new framework modeling method and Rietveld refinement of synchrotron powder diffraction data. *Zeolites* 1991; **11**: 502–6.
116. Baerlocher C, McCusker LB and Olson DH. *Atlas of Zeolite Framework Types*. Amsterdam: Elsevier, 2007.
117. Lv J, Sun Y and Liu H *et al.* Theory-orientated discovery of high-temperature superconductors in superhydrides stabilized under high pressure. *Matter Radiat Extremes* 2020; **5**: 068101.